

# Mechanical Properties of Borosilicate Glass Coated with Two-layered Ceramics by Sputtering

Toshihiko Hoshide and Takafumi Otomo

(Submitted July 26, 2006; in revised form March 23, 2007)

The durability of coated glass materials should be improved in their applications, and the possibility of a two-layer coating was examined as a processing for the improvement. In the present work, the borosilicate glass was coated with two-layered ceramics by the radio-frequency (RF) magnetron sputtering method, and mechanical properties of coated glass materials were investigated. The measured surface roughness and porosity of coating film suggested that relatively smooth and dense coating films were formed under the sputtering condition adopted in this work. Thicker film was found to be harder because of the avoidance of effect due to softer glass substrate. Higher RF output power resulted in harder film. The bending strength was reduced by longer time of sputtering as well as porosity of coating film. By comparison with glass materials coated with single ceramics and the glass substrate, it was clarified that the strength and hardness of coated glass materials were improved by two-layer coating.

**Keywords** alumina, borosilicate glass, coated glass materials, mechanical properties, silicon carbide, sputtering, two-layer coating

bending tests of the coated materials were conducted instead of tensile tests in this work. Finally, the dependencies of mechanical properties of coated materials on the thickness of two-layered ceramic film and on the RF output power were investigated to clarify a suitable sputtering condition.

## 1. Introduction

Glass materials coated with ceramic materials by sputtering are needed for various engineering applications. Recent works reported that glass sputtered with ceramic thin film is functionally used as magnetic/electronic device materials (Ref 1-3) as well as optical ones (Ref 1, 4-7). In functional and/or mechanical applications of coated glass materials, serious damages, which may be caused by unexpected forces in anomalous operations or the inconsistency in their equipping, are anticipated. Consequently, to improve the durability in their practical applications, the structural design of systems using coated glass materials requires a good understanding of their mechanical properties.

In the present work, mechanical properties of a borosilicate glass coated with alumina and silicon carbide were experimentally investigated to clarify the effect of two-layer coating. A radio-frequency (RF) magnetron sputtering method was adopted in producing thin ceramic films on glass. Coated glass materials were prepared by changing a combination of RF output power and film thickness. Hardness of coated glass is an important factor for tribological use (Ref 8), and the information on material strength is also required to guarantee the integrity during service. Hardness tests were carried out for coating film and the substrate glass. Since tensile tests of brittle glass or ceramic materials are very difficult to be performed to evaluate their strength characteristics adequately (Ref 9),

## 2. Experimental Procedures

### 2.1 Material Processing

A commercial borosilicate glass was used as a substrate material. Alumina ( $\text{Al}_2\text{O}_3$ ) of 99.99% purity and silicon carbide (SiC) of 99.8% purity were adopted as target materials. The geometry of glass substrate was a disk type with a diameter of 100 mm and a thickness of 2 mm. In coated materials,  $\text{Al}_2\text{O}_3$  film was first coated on the substrate glass, and afterward SiC-film was coated on  $\text{Al}_2\text{O}_3$ -coated materials. This order of coating has an advantage in tribological aspect because SiC is harder than  $\text{Al}_2\text{O}_3$ . In the present work, the thickness  $t_f$  of each ceramic film was selected to be 1 or 5  $\mu\text{m}$ , and four combinations of film thickness of respective ceramics were investigated as two-layered coating.

An RF magnetron sputtering apparatus of upper deposit type was used in the coating process. The distance between substrate and target materials was 40 mm in this apparatus. Metallic supporting or bonding plates, on which substrate and target materials were fixed, respectively, were being water-cooled during the processing. Before starting a steady sputtering, presputtering was carried out for 300 s so that a contaminated layer of target material could be removed. The initial degree of vacuum in a processing chamber was kept less than  $1.3 \times 10^{-4}$  Pa. The flow-rate of argon gas activating the sputtering process in the chamber was controlled to be 167  $\text{mm}^3/\text{s}$ , and the gas pressure in the chamber was set to be 1.3 Pa. In sputtering of ceramic target materials, the initial temperature of substrate was not controlled, and two levels of RF output power  $P_{\text{RF}}$  were selected as  $P_{\text{RF}} = 400$  and 600 W.

Toshihiko Hoshide and Takafumi Otomo, Department of Energy Conversion Science, Graduate School of Energy Science, Kyoto University, Yoshida-Honmachi, Sakyo-ku, Kyoto 606-8501, Japan. Contact e-mail: toshi.hoshide@ecs.mbox.media.kyoto-u.ac.jp.

## 2.2 Measurements of Film Surface Characteristics

Images of surface-areas in each coating film were taken through a laser-scanning microscope, and the images were processed into digital data by using a personal computer in which software for image-processing was installed. Data in individual areas on a coating film were used to evaluate roughness and porosity of respective areas, and the roughness and porosity were finally obtained as their averaged values for the coating film. By using the images processed by the software, the surface roughness  $R_a$  was evaluated as the center-line-average roughness.

In evaluating the porosity, the porosity  $p$  of a coating film was defined as a fraction of total pore-areas in the measured surface region. Pores in the measured surface-area were identified by an automatic threshold operation in the image-processing software.

From tribological aspect, the surface hardness of coated materials should be adequately evaluated. To avoid the influence of the substrate hardness on the film hardness, it has been revealed that a penetrating depth of indenter should be kept one-tenth or one-fifth of the film thickness (Ref 10). For this situation, a dynamic microhardness tester with the applicable range of indentation force from 98  $\mu\text{N}$  to 1.96 N is appropriate to measure the film hardness. By using a dynamic microhardness tester, the aforementioned condition is properly satisfied in ceramics-coated materials (Ref 11, 12).

## 2.3 Bending Test

For bending tests, plate type specimens with dimensions of 10 mm in width and 40 mm in length were cut out from coated materials and the glass substrates.

In evaluating bending strength, a three-point or four-point bending test is usually adopted. In this work, a three-point bending test is used to achieve more reduction of friction points in a supporting system. The span length in three-point bending test was set to be 20 mm. The loading rate was controlled so

that the rate of nominal stress at the position subjected to the maximum tensile stress in a specimen should be 100 MPa/s. In setting a coated specimen on supporting equipment, the coated surface of the specimen was located in the tensile side. In total, 15 specimens were prepared for each sputtering conditions. All tests were carried out in an ambient atmosphere, i.e., at temperature of  $292 \pm 6$  K and in relative humidity of  $73 \pm 2\%$ . The bending strength of coated and non-coated specimens was calculated as the maximum nominal stress monitored at their final failures irrespective of the actual breaking points.

## 3. Experimental Results and Discussions

### 3.1 Characteristics of Coating Film

The center-line-average roughness  $R_a$  is measured on specimen surfaces coated with  $\text{Al}_2\text{O}_3$ -SiC. Mean values of measured roughness are summarized in Table 1, in which roughness of glass is also indicated for comparison. As a whole trend, the roughness  $R_a$  of coated surface increases with increasing the total thickness of coating layer, and the surface coated with higher RF output power  $P_{\text{RF}}$  is smoother than that coated with lower power. Compared with the surface roughness of glass, the surface coated with ceramics under any condition is clearly rougher than the glass surface. Table 2 presents the porosity  $p$  related with the film thickness  $t_{\text{AO}}$  and  $t_{\text{SC}}$ , and RF power  $P_{\text{RF}}$ . As seen in Table 2, the porosity becomes larger for higher  $P_{\text{RF}}$ . In this case, too, the porosity becomes larger for higher  $P_{\text{RF}}$ , though the porosity increases as the total film is thicker. Since the average of porosities of ceramic films is about  $1.5 \times 10^{-3}$ , sufficiently dense films are formed under the present sputtering conditions.

Dynamic hardness  $H_{\text{DU}}$  of coating film is listed in Table 3. As reference data, dynamic hardness of coated single SiC-film with a thickness of 5  $\mu\text{m}$  and the glass substrate is also shown in Table 4. It is seen that ceramic films coated under any

**Table 1 Surface roughness of SiC-films coated on  $\text{Al}_2\text{O}_3$ -coated glass**

$\text{Al}_2\text{O}_3$ film thickness $t_{\text{AO}}$ , $\mu\text{m}$	1	1	5	5	Glass
SiC-film thickness $t_{\text{SC}}$ , $\mu\text{m}$	1	5	1	5	
Mean roughness $R_a$ , $\mu\text{m}$	$P_{\text{RF}} = 400$ W	$3.65 \times 10^{-3}$	$3.94 \times 10^{-3}$	$3.84 \times 10^{-3}$	$3.35 \times 10^{-3}$
	$P_{\text{RF}} = 600$ W	$4.17 \times 10^{-3}$	$3.33 \times 10^{-3}$	$3.66 \times 10^{-3}$	$3.90 \times 10^{-3}$

**Table 2 Surface porosity of SiC-films coated on  $\text{Al}_2\text{O}_3$ -coated glass**

$\text{Al}_2\text{O}_3$ film thickness $t_{\text{AO}}$ , $\mu\text{m}$	1	1	5	5
SiC-film thickness $t_{\text{SC}}$ , $\mu\text{m}$	1	5	1	5
Mean porosity $p$	$P_{\text{RF}} = 400$ W	$1.03 \times 10^{-3}$	$1.21 \times 10^{-3}$	$1.11 \times 10^{-3}$
	$P_{\text{RF}} = 600$ W	$1.27 \times 10^{-3}$	$1.63 \times 10^{-3}$	$1.62 \times 10^{-3}$

**Table 3 Dynamic hardness of SiC-films coated on  $\text{Al}_2\text{O}_3$ -coated glass**

RF output power $P_{\text{RF}} = 400$ W				
$\text{Al}_2\text{O}_3$ film thickness $t_{\text{AO}}$ , $\mu\text{m}$	1	1	5	5
SiC-film thickness $t_{\text{SC}}$ , $\mu\text{m}$	1	5	1	5
Mean hardness $H_{\text{DU}}$ , GPa	3.45	4.04	3.59	4.53
Coefficient of variation (COV)	0.0864	0.0940	0.0798	0.0697
RF output power $P_{\text{RF}} = 600$ W				
$\text{Al}_2\text{O}_3$ film thickness $t_{\text{AO}}$ , $\mu\text{m}$	1	1	5	5
SiC-film thickness $t_{\text{SC}}$ , $\mu\text{m}$	1	5	1	5
Mean hardness $H_{\text{DU}}$ , GPa	3.62	4.42	4.31	6.12
Coefficient of variation (COV)	0.0795	0.0451	0.0795	0.0648

condition are harder than the glass substrate. As a whole trend, thicker film has higher hardness, because the effect of the substrate, which is softer than SiC-film (see Table 4), becomes smaller in thicker film. For higher RF power  $P_{RF}$ , the surface hardness of coated materials is found to be larger. It is suggested that higher RF power brings in denser film. On the other hand, the hardness of SiC-film coated on  $Al_2O_3$ -coated glass is lower than that of coated single SiC-films. This is associated with an experimental observation (Ref 13) that  $Al_2O_3$ -film is softer than SiC-film. In Tables 3 and 4, the coefficient of variation, which is defined as the standard deviation divided by the mean value, is also indicated as a reference factor of statistical scatter. Comparing the coefficient of variation in Tables 3 and 4, hardness scatter of two-layered ceramics is found to be smaller than those of glass substrate and coated single SiC-film.

### 3.2 Bending Strength of Coated Material

Figure 1 presents strength distributions plotted on Weibull probability paper. As seen in Fig. 1, the strength distribution of

**Table 4 Dynamic hardness of single SiC-film coated on glass and glass substrate**

RF output power $P_{RF}$ , W	400	600	Glass
SiC-film thickness $t_{SC}$ , $\mu m$	5	5	
Mean hardness $H_{DU}$ , GPa	6.52	6.71	3.33
Coefficient of variation (COV)	0.143	0.168	0.123

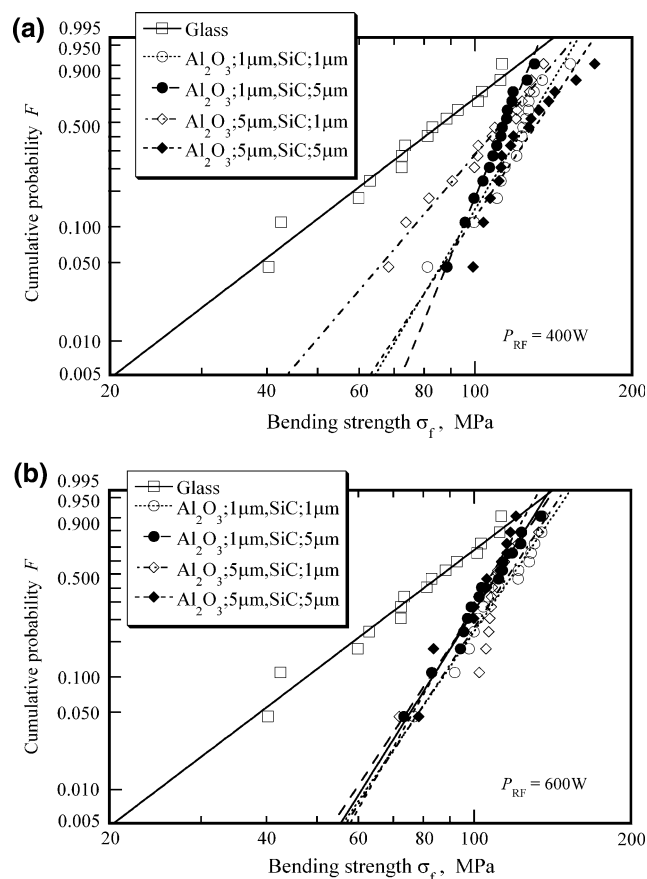


**Fig. 1** Weibull plot of distribution of bending strength

material coated under each condition shifts toward higher strength region compared with the strength distribution of the glass substrate. To obtain the shape parameter as a reference index of scatter, the strength distribution is approximated by using two-parameter Weibull distribution function  $F(\sigma_f)$  as

$$F(\sigma_f) = 1 - \exp \left\{ - \left( \frac{\sigma_f}{\beta} \right)^\alpha \right\} \quad (\text{Eq 1})$$

In the above equation,  $\alpha$  and  $\beta$  are, respectively, the shape and scale parameters. Each straight line in Fig. 1 presents the line drawn by fitting the strength data to Eq 1. Except for the strength data of the film with 5  $\mu m$   $Al_2O_3$  and 5  $\mu m$  SiC under  $P_{RF} = 400$  W and that with 5  $\mu m$   $Al_2O_3$  and 1  $\mu m$  SiC under  $P_{RF} = 600$  W, the strength data are well fitted by Eq 1. The exceptional strength data as mentioned above are well fitted by three-parameter Weibull distribution function rather than Eq 1.

The mean strength  $\sigma_{fm}$  with  $\alpha$  and  $\beta$  are indicated in Table 5. In respective materials coated under  $P_{RF} = 400$  and 600 W, generally, the mean strength decreases as the total thickness of coating film becomes thicker. However, the dependence of the mean strength on the difference in RF output is not so remarkable. Table 6 summarizes the strength characteristics in the material coated with single ceramics, i.e.,  $Al_2O_3$  or SiC, as well as the glass substrate. The comparison of strength between the coated materials and the glass substrate shows that the strength is generally improved by ceramics-coating. Especially, two-layer coating is found to raise the mean strength by comparing with the strength of single-ceramics coated material, except for the case of SiC-coating under  $P_{RF} = 600$  W.

The coefficient of variation (COV) and the shape parameter  $\alpha$  are associated with the scatter range of strength; smaller COV or larger  $\alpha$  corresponds to smaller scatter. The variations of COV and  $\alpha$ -value are large in materials coated under  $P_{RF} = 400$  W, though the values of COV and  $\alpha$  hardly change in the case of  $P_{RF} = 600$  W. By comparing the values of COV and  $\alpha$  in Tables 5 and 6, smaller COV and larger  $\alpha$  are seen in two-layered ceramics coated materials compared with their values in the glass substrate and single-ceramics coated materials. This implies that the strength scatter is reduced by two-layer coating.

Consequently, the improvement in strength properties, i.e., the increase in mean strength and the decrease in strength scatter, is expected by two-layer coating.

### 3.3 Relations between Strength and Other Parameters

Figure 2 presents the strength correlated with the porosity on the surface of coating. Although the range of porosity variation is narrow, the porosity has a bit of influence on the strength; i.e., a larger porosity degrades the mean strength. This is associated with the fact that surface pores sometimes act as defects dominating the strength in brittle materials.

As seen in Fig. 3, the strength is not improved even if the coating film becomes harder. This implies that the increase in film hardness hardly affect the improvement of strength of coated materials.

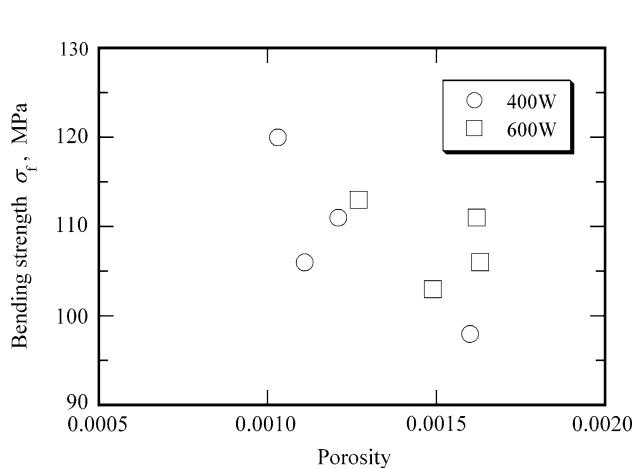
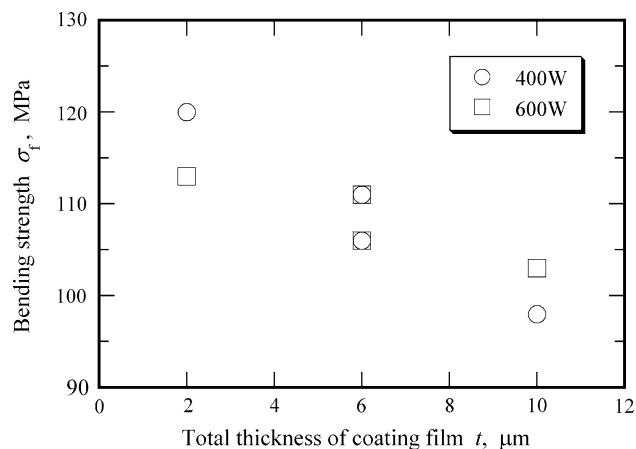
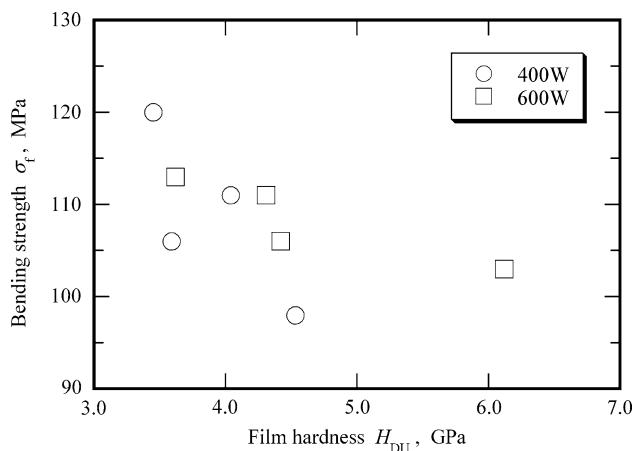
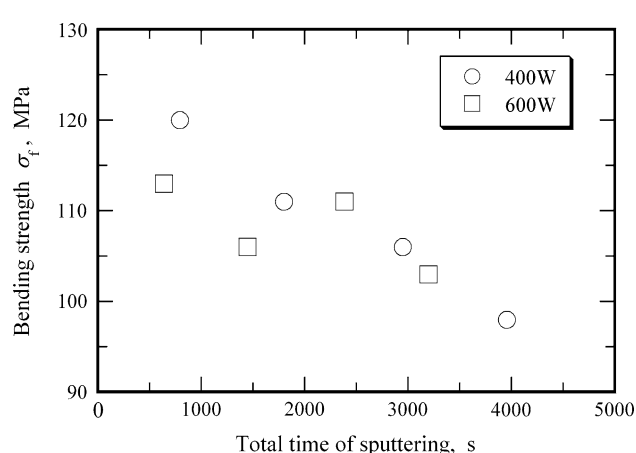
The strength is related with the total thickness of coating film in Fig. 4. The figure shows that the strength is reduced as the total thickness is increased. Note that the film formation rate depends on the target material even if the RF output is the same. By considering the point, the strength is correlated with the total time required for specified coating thickness. Figure 5 indicates the relation between the strength and the total time of

**Table 5 Bending strength of SiC-Al<sub>2</sub>O<sub>3</sub>-coated glass**

RF output power $P_{RF} = 400$ W				
Al <sub>2</sub> O <sub>3</sub> film thickness $t_{AO}$ , $\mu\text{m}$	1	1	5	5
SiC-film thickness $t_{SC}$ , $\mu\text{m}$	1	5	1	5
Mean strength $\sigma_{fm}$ , MPa	120	111	106	125
Coefficient of variation (COV)	0.134	0.0988	0.194	0.159
Shape parameter $\alpha$	8.36	11.5	5.60	7.68
Scale parameter $\beta$ , MPa	127	115	114	104
RF output power $P_{RF} = 600$ W				
Al <sub>2</sub> O <sub>3</sub> film thickness $t_{AO}$ , $\mu\text{m}$	1	1	5	5
SiC-film thickness $t_{SC}$ , $\mu\text{m}$	1	5	1	5
Mean strength $\sigma_{fm}$ , MPa	113	106	111	103
Coefficient of variation (COV)	0.155	0.153	0.132	0.129
Shape parameter $\alpha$	7.16	7.28	8.92	8.69
Scale parameter $\beta$ , MPa	120	112	117	109

**Table 6 Bending strength of Al<sub>2</sub>O<sub>3</sub>- and SiC-coated glass, and non-coated glass**

RF output power $P_{RF}$ , W	400		600		Glass
Al <sub>2</sub> O <sub>3</sub> film thickness $t_{AO}$ , $\mu\text{m}$	5	0	5	0	
SiC-film thickness $t_{SC}$ , $\mu\text{m}$	0	5	0	5	
Mean strength $\sigma_{fm}$ , MPa	81.1	76.0	81.0	110	79.9
Coefficient of variation (COV)	0.376	0.371	0.243	0.204	0.283
Shape parameter $\alpha$	3.18	2.93	4.18	4.88	3.70
Scale parameter $\beta$ , MPa	84.4	84.8	89.1	119.3	88.5

**Fig. 2** Bending strength correlated with porosity of coating film**Fig. 4** Relation between bending strength and total thickness of coating film**Fig. 3** Relation between bending strength and film hardness**Fig. 5** Relation between bending strength and total time of sputtering



sputtering. As seen in Fig. 5, the strength decreases for longer sputtering time irrespective of the RF output. Longer sputtering time brings the elevation of temperature of coated material, which results in the softening of glass substrate. The glass softening has been observed in such a heat treatment as elevating the initial substrate temperature (Ref 13).

Consequently, the strength variation depending on sputtering condition is primarily associated with the strength reduction of the substrate glass subjected to longer time at elevated temperature during sputtering process. Secondly, the coating film degradation due to porosity may affect the strength of coated materials. Of course, the bending strength may be affected by thermal stress due to a mismatch of linear expansion coefficient between glass substrate and ceramic film. At present, however, it is difficult to evaluate the thermal stress in coated materials because the substrate and film are not jointed as bulk materials. To clarify the effect of mismatch of linear expansion coefficient, the interface between bulk substrate and coated film on fracture surface should be investigated more minutely in future.

## 4. Conclusion

The improvement in durability of coated glass is desired in practical applications of such a material. In this work, two-layer coating was evaluated as a technique for the improvement of mechanical properties of coated glass. To investigate the effect of two-layer coating, the borosilicate glass was actually coated with two-layered ceramics consisting of alumina and silicon carbide. The coating was processed by the RF magnetron sputtering method under two different RF output powers. Mechanical properties of coated materials were investigated with respect to the sputtering condition. By measuring surface roughness and porosity on coating film, it was found that relative smooth and dense coating films were produced irrespective of the sputtering condition examined in this work. The hardness of coating film was measured by using a dynamic microhardness tester. Hardness test revealed that the coating film became harder for thicker film and/or higher RF output power. Strength tests of coated materials were also conducted under three-point bending mode. The strength properties of two-layer coated materials were improved in comparison with those of materials coated with single ceramics and of the glass substrate. In thicker films, the strength was reduced, though the film hardness became higher. The strength of coated materials was determined primarily by the total time of sputtering and second by the porosity of coating film; i.e., the strength degradation was brought by longer sputtering time and larger film porosity.

Consequently, it was suggested that mechanical properties of ceramics-coated material could be improved by sputtering process using two-layer coating with increasing RF output power.

## Acknowledgment

This work was supported by Grant-in-Aids for Scientific Research (C) (No. 18560078) from Japan Society for Promotion of Science.

## References

1. K.H. Kim, K.C. Park, and D.Y. Ma, Structural, Electrical and Optical Properties of Aluminum Doped Zinc Oxide films Prepared by Radio Frequency Magnetron Sputtering, *J. Appl. Phys.*, 1997, **81**(2), p 7764–7772
2. Y. Fukuma, H. Asada, N. Nishimura, and T. Koyanagi, Ferromagnetic Properties of IV-VI Diluted Magnetic Semiconductor  $\text{Ge}_{1-x}\text{Mn}_x\text{Te}$  Films Prepared by Radio Frequency Sputtering, *J. Appl. Phys.*, 2003, **93**(7), p 4034–4039
3. Y. Peng, C. Park, and D.E. Laughlin,  $\text{Fe}_3\text{O}_4$  Thin Films Sputter Deposited from Iron Oxide Targets, *J. Appl. Phys.*, 2003, **93**(10), p 7657–7959
4. D.-A. Chang, P. Lin, and T.-Y. Tseng, Optical Properties of  $\text{ZrTiO}_4$  Films Grown by Radio-Frequency Magnetron Sputtering, *J. Appl. Phys.*, 1995, **77**(9), p 4445–4451
5. G.T. Kiehne, G.K.L. Wong, and J.B. Ketterson, Optical Second-Harmonic Generation in Sputter-Deposited AlN Films, *J. Appl. Phys.*, 1998, **84**(11), p 5922–5927
6. H. Mizoguchi, N. Kitamura, K. Fukumi, T. Mihara, J. Nishii, M. Nakamura, N. Kikuchi, H. Hosono, and H. Kawazoe, Optical Properties of  $\text{SrMoO}_3$  Thin Film, *J. Appl. Phys.*, 2000, **87**(9), p 4617–4619
7. S. Venkataraj, O. Kapperiz, H. Weis, R. Drese, R. Jayavel, and M. Wuttig, Structural and Optical Properties of Thin Zirconium Oxide Films Prepared by Reactive Direct Current Magnetron Sputtering, *J. Appl. Phys.*, 2002, **92**(7), p 3599–3607
8. T.W. Scharf, R.D. Ott, D. Yang, and J.A. Barnard, Structural and Tribological Characterization of Protective Amorphous Diamond-Like Carbon and Amorphous  $\text{CN}_x$  Overcoats for Next Generation Hard Disks, *J. Appl. Phys.*, 1999, **85**(6), p 3142–3154
9. T. Hoshide, Strength Characteristics of Structural Ceramics, *Mater. Sci. Res. Int.*, 1996, **2**(4), p 220–228
10. P.J. Burnett and D.S. Rickerby, Assessment of Coating Hardness, *Surf. Eng.*, 1987, **3**(1), p 69–76
11. T. Hoshide, K. Hayashi, T. Saito, K. Katsuki, and T. Inoue, Mechanical Properties of Borosilicate Glass Coated with Alumina by Sputtering Process, *Mater. Sci. Res. Int.*, 1996, **2**(1), p 33–38
12. T. Hoshide, A. Nebu, and K. Hayashi, Bending Strength of Borosilicate Glass Coated with Alumina and Silicon Carbide by RF Magnetron Sputtering, *JSME Int. J., Ser. A*, 1998, **41**(1), p 332–337
13. T. Hoshide and M. Akamatsu, Mechanical Properties of Borosilicate Glass Coated with Pure Aluminium by Sputtering Process, *J. Mater. Eng. Perform.*, 2004, **13**(5), p 588–592